C T Sci ...

JPL NO. 9950-541

DOE/JPL 954685-81/4
Dist. Catagory UC-63

STUDY OF THE EFFECTS OF IMPURITIES ON THE PROPERTIES OF SILICON MATERIALS AND PERFORMANCE OF SILICON SOLAR CELL

FOURTH ANNUAL TECHNICAL REPORT

March 1981

By C. T. Sah

Contract No. 954685

The JPL Low Cost Solar Array Project is sponsered by the U. S. Dept. of Energy and forms a part of the Solar Photovoltaic Conversion Program to initiate a major effort toward the development of low-cost solar arrays. This work was performed for the Jet Propulsion Laboratory, California Institute of Technology by agreement between NASA and DOE.

(NASA-CR-164452) STUDY OF THE EFFECTS OF IMPURITIES ON THE PROPERTIES OF SILICON MATERIALS AND PERFORMANCE OF SILICON SOLAR CELL Annual Technical Report (California Inst. of Tech.) 30 p HC A03/MF A01 CSCL 10A G3/44

N81-25494

Unclas 26602

DOE/JPL-954685-81/1
Dist. Catagory UC-63

STUDY OF THE EFFECTS OF IMPURITIES ON THE PROPERTIES OF SILICON MATERIALS AND PERFORMANCE OF SILICON SOLAR CELL

FOURTH TECHNICAL REPORT

March 1981

By C. T. Sah

Contract No. 954685

The JPL Low Cost Solar Array Project is sponsered by the U. S. Dept. of Energy and forms a part of the Solar Photovoltaic Conversion Program to initiate a major effort toward the development of low-cost solar arrays. This work was performed for the Jet Propulsion Laboratory, California Institute of Technology by agreement between NASA and DOE.

TECHNICAL CONTENT STATEMENT

NEW TECHNOLOGY

No new technology is reportable for the period covered by this report.

TABLE OF CONTENT

LIST OF ILLUSTRATIONS

LIST OF TABLES

ABSTRACT

Semiconductor material cost is one of the factors which determines the performance-cost ratio and economical feasibility of silicon solar cells for terrestrial power generation. Decreasing the cell thickness would lower the silicon material cost. The energy conversion efficiency of a back-surface-field solar cell will have a peak as the silicon film thickness is reduced due to two opposing factors: - the open circuit voltage increases and the short circuit current decreases with decreasing cell thickness. A computer-aided-design study is presented in this paper on the dependence of this efficiency peak on the concentrations of the recombination and dopant impurities. The illuminated current-voltage characteristics of over 100 cell designs were obtained using the transmission line circuit model to numerically solve the Shockley Equations. Using an AM1 efficiency of 17% as a target value, which is the highest encapsulated silicon cell efficiency used in the Block IV modules of the Low-Cost Solar Array Project,* it is shown that the efficiency versus thickness dependence has a broad maximum which varies less than 1% over more than three-to-one range of cell thickness from 30 to 100 μm. Optical reflecting back surface will give only a slight improvement of AM1 efficiency, about 0.7%, in this thickness range. The sensitive dependence of efficiency on patchiness across the back-surface-field low-high junction in thin cells is noted.

---

* This figure was given on p.21 of JPL/DOE 5101-143, a report distributed at the 14th Photovoltaic Specialist Conference, January, 1980.

I. INTRODUCTION

The objective of this program is to determine the effects of impurities and defects on the performance and permanence of silicon solar cells. It includes computer-aided theoretical and experimental studies of the effects of impurities on the properties of silicon intentionally doped with specific impurity elements, and the effects of these impurities on the impurity related energy level positions, the concentrations of these energy levels and the recombination-generation rates of electrons and holes at these energy levels.

This fourth technical report contains a theoretical analysis of the dependence of silicon solar cell performance on the thickness of the cell and on the concentration of the recombination impurity in high efficiency cells, such as those used in the Block IV module of the Low-Cost Solar Array Projects which have AM1 efficiencies as high as 17%.[#]

Other studies, still incomplete and not reported here, include the effects of random perimeter and bulk defects and impurities on the open circuit voltage of back-surface-field cells, a comparison of theory with experimental thin film n+/p/p+ dendritic web cells from zinc vapor reduced silicon, measurements of the thermal capture rates of electrons and holes at the Titanium recombination levels by the capacitance transient spectroscopy method, performance limits from intrinsic and residual defect-impurity complexes in high efficiency cells and others. Accurate recombination rate data of other impurities (Mo, V and others) are also needed to predict their maximum allowable densities for the optimum cell designs (thickness and diffusion profiles) to get the best performance-cost ratio as well as the highest permanence.

Reported on p.21 of JPL/DOE 5101-143, a report distributed at the 14th Photovoltaic Specialist Conference, January 1980.

II. EFFECT OF THICKNESS ON SILICON SOLAR CELL EFFICIENCY

2.1 INTRODUCTION

One of the factors which determines the economic feasibility of a solar cell is the cost of the semiconductor material. Thus, cells made on thin semiconductor films can lower the cost if the energy conversion efficiency is maintained and if other manufacturing costs are not higher in the thin film technology.

Several factors determine performance or efficiency of a solar cell as the cell thickness is decreased. Less light is absorbed by the semiconductor film when its thickness decreases. This reduces the photon generated current or the short circuit current of the solar cell which would decrease the power output and efficiency. However, if the loss of the photogenerated electron-hole pairs is mainly due to thermal recombination in the quasi-neutral base layer of the cell, then the base recombination loss would decrease when cell is thinner since the recombination volume is smaller. Decreasing the base recombination loss would increase the photon generated voltage or the open circuit voltage across the cell and increase the energy conversion efficiency. The back-surface-field cells with an n+/p/p+ or p+/n/n+ diffusion profile would limit the electron-hole recombination to the p-type or n-type base region and give the improvement of the open circuit voltage in thinner cells.

These two opposite effects from reduction of the cell thickness (decreasing short circuit current and increasing open circuit voltage) would give an optimum cell thickness at which the efficiency peaks. This optimum cell thickness is a function of the base recombination rate or the base recombination current density.

A third factor which would improve the performance-cost ratio in a thin cell is that its tolerance to the level of recombination impurity density may also be improved in two ways. First, thinner cells have a higher critical concentration of recombination impurity above which the cell efficiency would drop below an acceptable value since the efficiency begins to degrade substantially only when the base minority carrier diffusion length drops significantly below the cell thickness. A qualitative estimate is given by $L_B = \sqrt{D_B \tau_B} = \sqrt{D_B / c_T N_{TT}} < W_B$ or $N_{TT} > (D_B / c_m^t W_B^2)$ where N_{TT} is the recombination impurity concentration in the base, c_m^t is the thermal capture rate of minority carriers in the base (about 10^{-7} cm^3/sec), D_B is the minority carrier diffusion length in the base (about 10 cm^2/sec) and W_B is the base layer thickness. For a cell of 10 micron thick, the threshold recombination impurity concentration is about $N_{TT} > 10/(10^{-7} x 10^{-3x2}) = 10^{14}$ $atom/cm^3$ which is more than an order of magnitude higher than in thick cell such as 10^{12} Zn/cm^3 in a 300 μm Zn-doped cell [1]. Second, gettering of the recombination impurities by surface sinks, such as the high-concentration back surface field layer, should be much more effective than in thicker cells since the recombination impurity atoms in the thin base will have a much smaller distance to outdiffuse to reach the sink where they would contribute negligible base recombination current. Permanence should not be affected at normal cell operation temperatures (100°C or less) by indiffusion into the base of the outdiffused recombination impurities since outdiffusion or gettering is usually performed at high temperatures (above 900°C) while the diffusivity and thermal activation rate of the impurities in the sink layer are both extremely small at the operation temperatures. In addition, the sink layer could be removed during processing if necessary. The only possible detrimental effect is gettering of the recombination impurities by the diffused emitter which could significantly increase emitter recombination and offset the performance gain from lower base recombination.

2.2 MODEL OF THE SILICON SOLAR CELL

This section describes the computer models used in the numerical analyses such as the dopant and recombination impurity profiles, the recombination impurity parameters, the material parameters and the cell geometry (junction depth and layer thickness). Analyses of the computed cell performance of these cell designs are given in the next section.

The encapsulated silicon cells used in the Block IV modules of the Low-Cost Solar Array Project, have efficiencies from 12 to 17% for module price of \$7 to \$11.2 per peak watt.# For high efficiency cells (17%) to reach the 70 cents per peak watt 1986 DOE price goal for terrestrial power generation,# electron-hole recombination loss in the base region of the cell must be very low. Previous design calculations [1] showed that to achieve 17% AM1 efficiency, the cell should have a back-surface-field layer to prevent the photo-generated minority carriers in the base from reaching the back ohmic contact which has high recombination rate and it should also have a low concentration of recombination impurity centers in the base, $<10^{12}$ atom/cm^3, which corresponds to 100 μs lifetime and 300-400 μm diffusion length for minority carriers in the base.

Analytical solutions of cell performance cannot be obtained for these real cells due to (1) the complicated position dependences of the doping and diffusion impurity concentrations, the mobilities and diffusivities, the optical generation rate from solar illumination and (2) the nonlinear effects from trapped charges at the recombination impurity centers and from high injection level in the base which is indicated in Table I in the next section where the results are analyzed. In order to account for these effects in a real silicon cell, the six Shockley Equations are solved numerically by the transmission line circuit model method without any analytical approximations. This method was successfully used to predict the effect of zinc impurity on silicon cell performance [1]. This method is briefly reviewed in the following discussion.

Reported on p.2 and 21 of JPL/DOE 5101-143, a report distributed at the 14th Photovoltaic Specialist Conference, January, 1980.

The six Shockley Equations (two continuity equations, two current equations, one Poisson equation and one kinetic equation for the trapped electrons or holes at the recombination centers) for a one-level recombination center or the seven Shockley Equations for a two-level recombination center are first synthesized into a one-dimensional three-wire transmission line. The three wires correspond to the hole current line, the electron current line and the displacement current line whose potentials are the hole quasi Fermi potential, the electron quasi Fermi potential and the electrostatic potential respectively. The two-level recombination center model employed corresponds to zinc [1], gold, silver, titanium, vanadium, sulfur and many other metallic impurities. For each impurity, the appropriate thermal capture and emission rate coefficients must be used. There are four rates per energy level which consist of electron and hole capture and emission rates, c_n, c_p, e_n and e_p. The spatial dependence of the concentration of the recombination impurity can be varied in any arbitrary manner to correspond to the actual concentration profile in the cell. In this analysis, a spatially constant profile is assumed.

A two hundred (198) lumped-section transmission-line computer model is solved by conventional matrix inversion procedure to obtain the illuminated current-voltage characteristics. The front and back surfaces are assumed to be perfect ohmic contacts (short-circuiting the three wires of the transmission line at both ends). Both the n+/p/p+ and the p+/n/n+ diffusion profiles are analyzed. The emitter layer is assumed to be 0.25 μm thick and the back surface field layer is taken to be 1.0 μm thick. The n+ and p+ diffusion profiles are analytical fits to the experimentally measured profiles of phosphorus and boron diffusion described previously [1]. These are $1-X^{2/3}$ for the boron profile and $\exp(-X^6)$ for the phosphorus profile where X is the normalized distance.

Recombination parameters used in these analyses are those of the two zinc

levels used previously [1] for two reasons: first, these parameters of zinc are probably the most reliable among all the impurities in silicon and second, zinc is a major residue impurity in one of the alternative silicon purification processes for low cost solar cell manufacturing [2]. The results obtained for zinc should also be applicable to other impurity recombination centers in silicon solar cells since the general dependence of the efficiency and its peak location as a function of cell thickness should be relatively insensitive to the recombination parameters of the particular impurity used as a model.

Interband Auger recombination of electrons and holes is also included in the device model since it is one of the important performance limitations for high efficiency cells. The interband Auger recombination mechanism was also included in the previous analysis concerning the effect of zinc on silicon solar cell performance [1] but the numerical constants were inadvertently left out. These are $c^n = 2.8\text{x}10^{-31}$ cm^6/sec, $c^p = 9.9\text{x}10^{-32}$ cm^6/sec, $e^n = c^n n_i^2 = 2.8\text{x}10^{-11}$ sec^{-1} and $e_p = c^p n_i^2 = 9.9\text{x}10^{-11}$ sec^{-1} with $n_i = 1.0\text{x}10^{10}$ cm^{-3} at 297.2°K. The capture rates, c^n and c^p, were taken from the latest experimental data of Dziewior and Schmid [3].

The numerical values of the material parameters used in the computation, the choice of the variation of the thickness of each of the 198 lump sections, and the computation procedure were all discussed previously [1]. These are followed in the present calculation using a 25/50/73/50 four region computer model. The four regions are the emitter region, the junction space charge region, the quasi-neutral base region and the back surface field region. The numbers here indicate the number of lump sections used in each of the regions. The variation of the thickness of the lump sections is made reasonably smooth so that there is no more than a factor of three change between the thickness of the adjacent lumps. This rule is essential to get fast convergence and accurate results which was used in all the previous numerical analyses and was

arrived at by trial and error.

The only extension made in this analysis over the previous ones is the inclusion of a reflecting back surface (BSR) to simulate a two-optical-path cell design for cells with a reflecting substrate-semiconductor interface. The BSR structure has been suggested and used by many workers in thin cells to increase the short circuit current. For very thin cells (around a micron thick film), perfectly reflecting back surface can increase the short circuit current by as much as a factor of two in the limit. In this analysis, computations are made to determine if the reflecting back surface will significantly affect the cell performance for thin cells with peak-efficiency thickness. It does not.

The distributed volume photocurrent generators, located at position x_1 and driving the lump section between x_1 and x_2, are given below. For one optical path (perfectly transmitting back surface), it was given by [1]

$$J_0(x_1) = (x_2-x_1)^{-1}\, q\int_{\lambda_0}^{\lambda_\infty}(\lambda/hc)P(0,\lambda)[e^{-\alpha x_1} - e^{-\alpha x_2}]d\lambda.$$

For two optical paths with a back surface reflectivity of $R_L(\lambda)$ and cell thickness of L, it is given by

$$J_0(x_1) = (x_2-x_1)^{-1}\, q\int_{\lambda_0}^{\lambda_\infty}(\lambda/hc)P(0,\lambda)\{e^{-\alpha x_1} - e^{-\alpha x_2} + R_L[e^{-\alpha(2L-x_2)} - e^{-\alpha(2L-x_1)}]\}d\lambda$$

Here, $P(0,\lambda)$ is the incidence solar spectral irradiance, $\alpha(\lambda)$ is the absorption coefficient of silicon, λ_∞ is the cutoff wavelength of silicon (λ=hc/E_G) and λ_0 the cutoff wavelength of the solar spectrum. The front surface is assumed to be perfectly transmitting, i.e. with a perfect anti-reflection coating. For a bare silicon surface, the integrand above would contain an additional factor of $[1 - R(\lambda)]$ where $R(\lambda)$ is the front surface reflectivity of bare silicon. The three parameters, $P(0,\lambda)$, $\alpha(\lambda)$ and $R(\lambda)$, are tabulated in our previous paper [1].

2.3 DISCUSSION OF COMPUTED RESULTS

The effects of thickness on the cell performance are computed for both the n+/p/p+ and p+/n/n+ cells with uniform zinc recombination center density under one-optical-path (no back surface reflection) and two-optical-path (perfect back surface reflection) conditions and for a perfect anti-reflection coated front surface. These are given as families of curves with substrate doping as the constant parameter. More than 100 cells were computed and each cell gives one point on these curves. A complete illuminated I-V curve takes about 60 seconds CPU time on a CYBER-175 time sharing computer with detailed outputs of the internal characteristics (electron, hole, trapped charge and net charge densities, electric field and electrostatic potential and quasi-Fermi potential variations with position). At each illumination or voltage conditions, five to eight iterations through the 198 sections are required to reach convergence. A simple initial guess of the equilibrium electrostatic potential would require as much as 15 iterations to reach convergence.

Families of AM1 efficiency are shown in Figure 1 for a constant base dopant impurity concentration of $5x10^{14}$ atom/cm^3 which corresponds to 25 ohm-cm p-type silicon and 10 ohm-cm n-type silicon. The numerical labels of the curves have the following meaning. The first two digits are substrate dopant concentration, for example, $54=5x10^{14}$ cm^{-3}. The third and fourth digits are for the zinc or recombination impurity concentration, for example, $12=1.0x10^{12}$ Zn/cm^3. The fifth digit is the number of optical path, for example, 1 is for one pass and 2 for two passes or perfect reflecting back surface. The last character, a letter, denotes the conductivity type of the base, for example, p is for p-type base and n is for n-type base.

The following results are evident from the families of curves in Fig. 1 which are numerically listed and discussed.

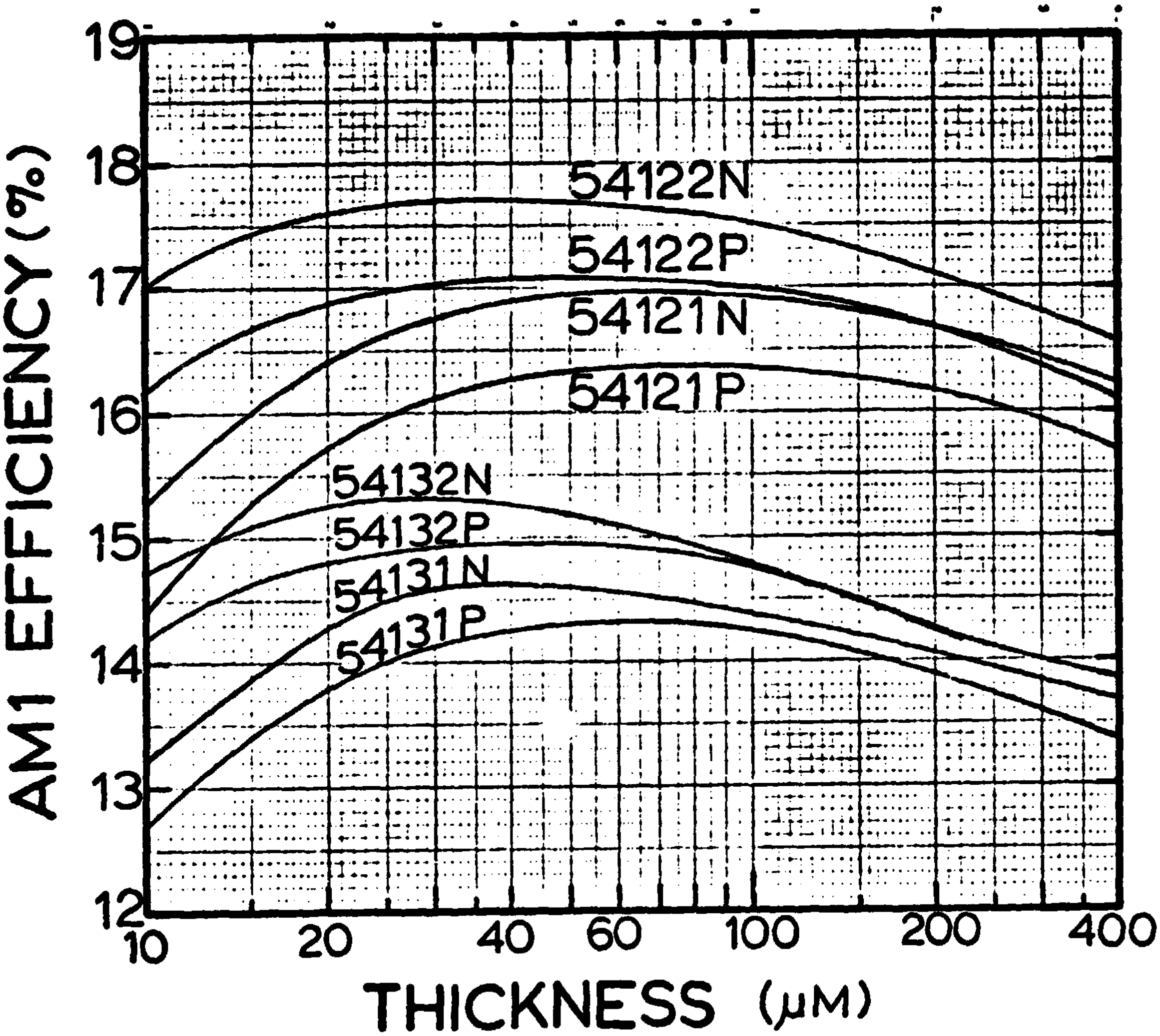

Figure 1 AM1 efficiency versus thickness of silicon n+/p/p+ (P) and p+/n/n+ (N) silicon solar cells with base doping of $5x10^{14}$ cm^{-3} and recombination impurity concentrations of 10^{12} or 10^{13} Zn/cm^3.

TABLE 1 MID-EMITTER AND MID-BASE LIFETIMES AND CARRIER CONCENTRATIONS IN ZINC DOPED SILICON p+/n/n+ and n+/p/p+ SOLAR CELLS UNDER ONE AM1 SUN ILLUMINATION.

Cell Type		p+/n/n+	n+/p/p+
Computer Run Numbers		54121N RUN824	54121P RUN809
Cell Thickness (μm)		250	250
Base Dopant Density (cm^{-3})		5.0E+14	5.0E+14
Emitter Impurity Diffusion Profile (cm^{-3})		2.5E+20 $*[1 - X^{2/3}]$	2.5E+20 $*[\exp(-X^6)]$
Emitter Junction (μm)		0.25	0.25
Auger Capture Rates (cm^6/s)		$c^n = 2.8E-31$	$c^p = 9.9E-32$
Mid-emitter Minority Carrier Thermal and (Auger) Lifetimes μs/(ps)	SC	50.0(773)	16.82(63.7)
	MP	50.0(773)	16.82(63.7)
	OC	50.0(773)	16.82(63.7)
Mid-base Minority and (Majority) Carrier Lifetimes (μs)	SC	60.3(64.6)	89.60(89.60)
	MP	60.9(62.5)	88.24
	OC	65.2(65.4)	78.89
Mid-base Minority and (Majority) Carrier Densities (cm^{-3})	SC	1.14E+13 (5.12E+14)	5.00E+12 (5.08E+14)
	MP	3.98E+13 (5.37E+14)	4.24E+13 (5.45E+14)
	OC	5.31E+14 (1.03E+15)	6.15E+14 (1.12E+15)
JSC (mA/cm^2)		32.32	31.44
VOC (mV)		577.96	579.34
FF		0.7882	0.7846
EFF (%)		16.559	16.073

(1) Location of the Efficiency Peak

All of the curves show an efficiency peak, confirming the physical picture discussed earlier in which V_{OC} increases and J_{SC} decreases with decreasing cell thickness. An important feature is that the efficiency peak is very broad, covering as much as a three-to-one range in thickness. For example, the curve 54122P for a family of n+/p/p+ cells with $N_{AA}=5x10^{14}$ cm^{-3} base doping, $N_{TT}=1x10^{12}$ Zn/cm^3 recombination impurity concentration, and a perfect reflecting back surface to give two optical passes, shows an efficiency of more than 17% for cell thickness from 27 to 100 μm and the peak is 17.09% at 60 μm thickness.

(2) Comparison of n+/p/p+ and p+/n/n+ Cells

p+/n/n+ cells have higher efficiencies which peak at smaller cell thicknesses than the corresponding n+/p/p+ cells. For example, let us compare the two cell families, 54122N and 54122P, both having 10^{12} Zn/cm^3 and perfect reflecting back surface. The n-base cells, 54122N, peak at 17.7% and 35 μm cell thickness while the p-base cells, 54122P, peak at 17.1% and 50 μm cell thickness.

The higher efficiency of the n-base cell than the p-base cell was shown to be due to the lower interband Auger recombination rate of electrons in the p-type emitter because the boron emitter diffusion profile is much more gradual (given by $1 - X^{2/3}$) than the phophorus diffusion profile in the n-type emitter (given by $\exp[-X^6]$). The nearly constant phosphorus or electron concentration in the n-type diffused emitter gives a shorter hole lifetime in the emitter than the electron lifetime in the p-type diffused emitter. For example, the mid-emitter and mid-base lifetimes for the 250 μm thick cells 54121N and 54121P are tabulated in Table 1 for short circuit (SC), maximum power (MP) and open circuit (OC) conditions which also gives the carrier concentrations at the mid-base point to indicate the injection level.

The computer calculation results listed in this table show that the main difference is the higher emitter recombination lifetime of the p+/n/n+ cell, which is 773 ps at mid-emitter (0.10 μm from surface) and entirely due to interband Auger recombination, compared with that of the n+/p/p+ cell, which is 63.7 ps. The higher emitter recombination rate in the n+ emitter reduces the short-circuit current by 32.32-31.44=0.88 mA/cm^2 as indicated in Table 1. This reduction of short-circuit current due to higher interband Auger emitter recombination in the n+ emitter is the predominant factor which makes the n+/p/p+ cell slightly less efficient than the p+/n/n+ cell. It is evident that proper control of the emitter diffusion profile can reduce interband Auger recombination in the emitter layer and reverse the relative efficiency figures between the n+/p/p+ and the p+/n/n+ cells.

The example just given was for a relatively thick cell of 250 μm. The slightly better efficiency of p+/n/n+ cell than n+/p/p+ cell persists for thinner cells as evident by comparing the family of curves of the n-base cell with that of the p-base cell given in Figure 1. The reason is that high injection level condition already began for the thick cell, as reflected by the minority and majority carrier concentrations given in Table 1. Thus, for thinner base cells with smaller recombination volume, the injection level will increase with corresponding increase of the minority carrier lifetime in the base of the two type of cells to approach each other so that the small base lifetime difference, 61 μs (p+/n/n+) versus 88 μs (n+/p/p+) shown in Table 1, will diminish. The emitter layer, however, will stay at the low level condition since the majority carrier density in the emitter is so high. Thus, for thinner cells, we would expect the difference in emitter recombination between the p+/n/n+ and the n+/p/p+ cells to persist, favoring the p+/n/n+ cell. The highest efficiency (∿ 18%) was observed in p+/n/n+ silicon cells [4] which is consistent with the above analysis and further supports the

contention that emitter diffusion profile control can improve the short circuit current by reduction of the interband Auger recombination in the diffused emitter layer.

(3) Dependence of Recombination Impurity Density or Base Lifetime

Cells with lower recombination impurity density or larger base lifetime and hence higher efficiency have efficiency peaks at larger cell thickness. This is demonstrated in Figure 1. For example, the cell family of 54122N has an efficiency peak of 17.7% at 35 μm cell thickness while 54132N peaks at 15.3% and 25 μm cell thickness. This is qualitatively understood from the dependence of the open circuit voltage on cell thickness and base minority carrier diffusion length in a back surface field cell. The use of the BSF to increase the open circuit voltage is effective only when the diffusion length is large (lower recombination impurity concentration) or the cell thickness is small compared with the diffusion length. Thus, the open circuit voltage would begin increase at a smaller cell thickness if the diffusion length is small or the recombination impurity density is high, such as the cells with 10^{13} Zn/cm^3 (54131 and 54132 curves in Figure 1). This would move the efficiency peak to smaller cell thickness.

(4) Reflecting Back Surface or Two Optical Passes

Perfect back surface reflection (BSR) increases the efficiency as expected since it increases the short circuit current but BSR will also decrease the cell thickness where the efficiencv peaks. For example, 54122N (with BSR or two-pass) has a 17.7% peak efficiency at 35 μm thickness while 54121N (one-pass) has a 16.9% peak efficiency at 60 μm. BSR provides the largest improvement of cell performance for thin cells since it increases the available photo current or short circuit current by a factor of two over the one-pass non-reflecting back surface cells. The effectiveness of BSR decreases with increasing cell thickness as indicated by the curves given in Figure 1.

(5) Effect of Base Resistivity or Base Dopant Concentration

The effect of base resistivity or base dopant impurity concentration on the thickness dependence is shown in Figure 2 where the 55131P and 55131N curves are for cells with $5x10^{15}$ atom/cm^3 base dopant impurity concentration while the 54131P and 54131N curves are for $5x10^{14}$ atom/cm^3. It is evident that the peak efficiency occurs at about the same cell thickness for a particular cell type (n+/p/p+ type or p+/n/n+ type) and is relatively independent of the base dopant impurity concentration in this concentration range. This is consistent with the physical reasoning given in section (3) since the minority carrier diffusion length in the base is relatively insensitive to the base dopant concentration. We would only expect a small dependence on dopant impurity concentration since the mobility or diffusivity decreases with increasing dopant impurity concentration so that the diffusion length in the base is smaller at higher base dopant concentration. This would make the BSF less effective on increasing the open circuit voltage until the cell is very thin. Thus, increasing the base doping would move the efficiency peak to a smaller cell thickness but the peak would be expected to be very broad.

(6) Open Circuit Voltage (V_{OC})

The open circuit voltage increases with decreasing cell thickness as indicated in Figure 3. This is expected since thinner cells have smaller base recombination volume and hence require a higher junction voltage to produce the same recombination current to balance the photogenerated current. The rate of increase of V_{OC} with decreasing thickness is larger for lower base dopant impurity concentration as expected from the physical model of the effect of back surface field disucssed in sections (3) and (5). This is also evident in Figure 3 where the magnitude of the slope of 55131P ($5x10^{15}$ cm^{-3} base doping) is smaller than that of 54131P or 54121P ($5x10^{14}$ cm^{-3} base doping).

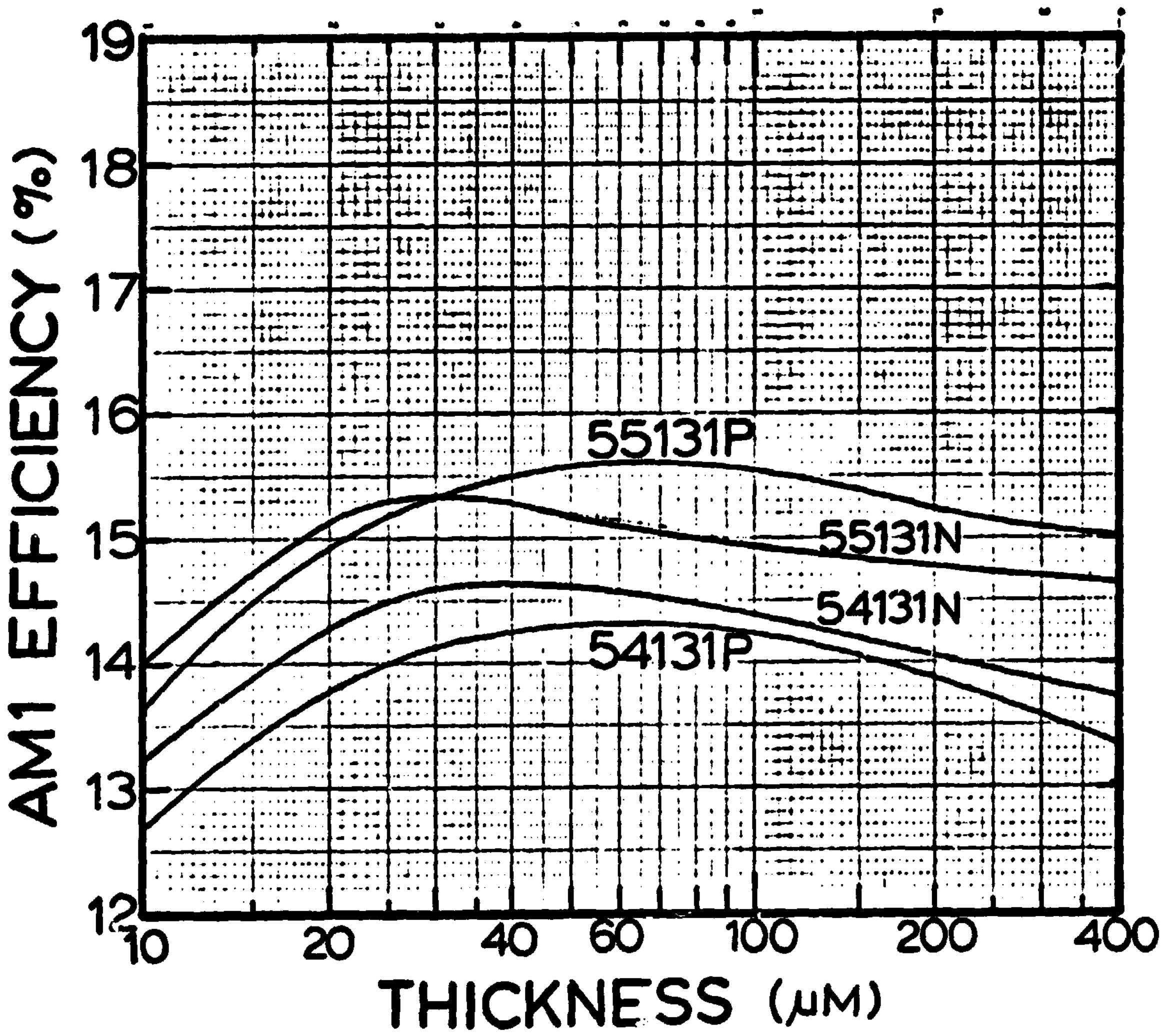

Figure 2 The thickness dependence of the AM1 efficiency of silicon p+/n/n+ and n+/p/p+ solar cells with the base dopant impurity concentration as the parameter.

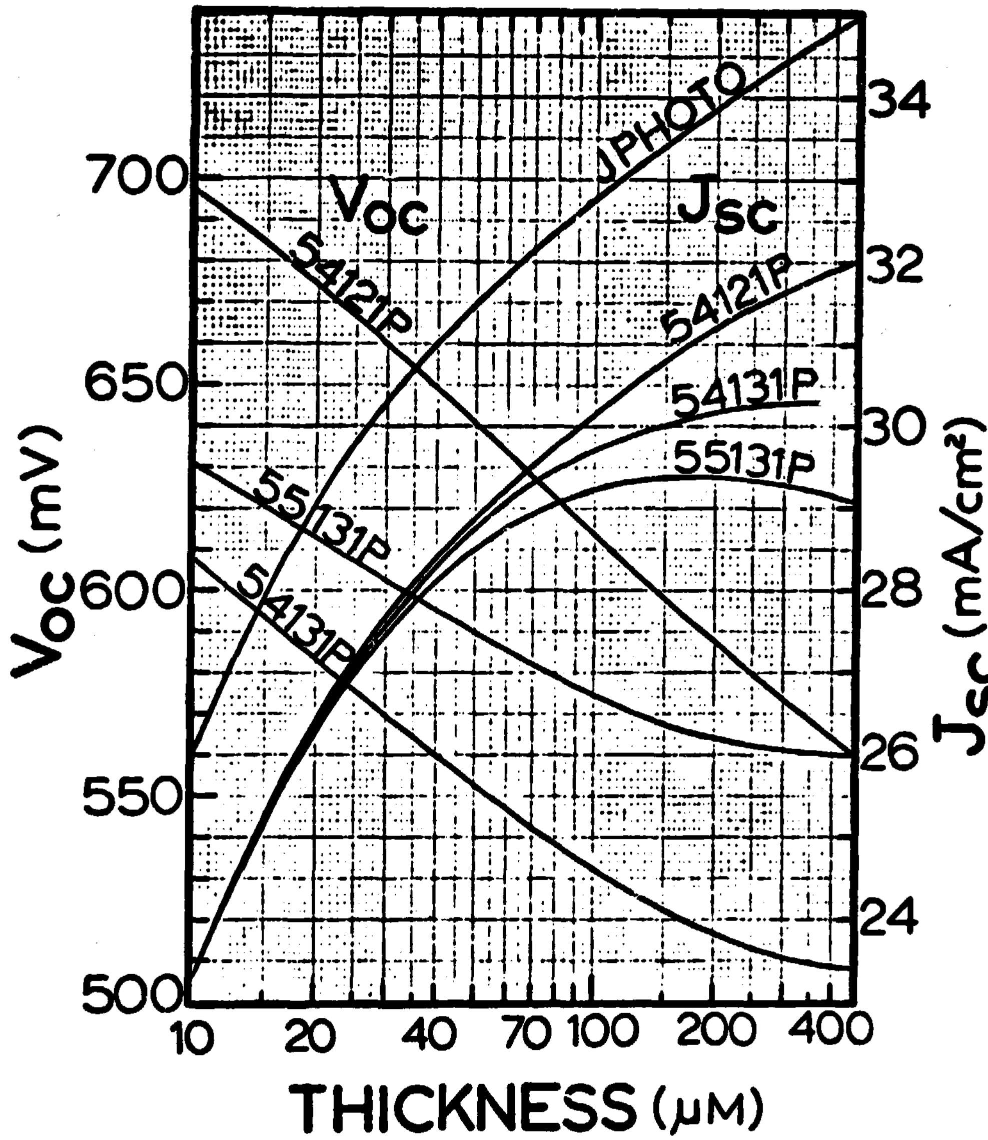

Figure 3 The open circuit voltage, V_{OC}, and the short circuit current, J_{SC}, as a function of thickness of silicon junction solar cells under one AM1 sun illumination.

The open circuit voltage is increased only slightly by adding a perfectly reflecting back surface. For example, V_{OC}=641.33 mV for 54121P and 643.21 mV for 54122P cells at 50 μm cell thickness. This shows an increase of only 1.92 mV from having two optical passes in the 54122P cell.

(7) <u>Short Circuit Current</u>, J_{SC}

The short circuit current decreases with decreasing cell thickness as indicated in Figure 3. This is expected since thinner cell has smaller volume to absorb the solar photons. For thin cells, J_{SC} is relatively independent of the densities of the dopant and recombination impurity as indicated by the three curves, 54121P, 54131P and 55131P. This is expected since for thin cells, recombination loss becomes less important and short circuit current is mainly determined by the number of photons absorbed in the entire cell. The collection efficiency approaches unity in thin cells which is so thin that the photo-generated electrons and holes will have no chance to recombine before being collected by the p/n junction.

Two optical passes using a perfectly reflecting back surface will increase J_{SC} by only a small amount around the efficiency peak at about 50 μm cell thickness. For example, the improvement is 30.146 - 28.888 = 1.258 mA/cm^2 in a 2-pass cell, 54122P, over the 1-pass cell, 54121P. The relative improvement of short-circuit-current in a 2-pass cell over a 1-pass cell is larger for thinner cells, but the efficiency would have dropped off significantly for very thin cells. For example, at 10 μm cell thickness, the increase of J_{SC} in the 2-pass cell, 54122N, over the 1-pass cell, 54121N, is 27.477 - 24.855 = 2.622 mA/cm^2, but the efficiency for the 2-pass cell is 0.7% smaller than the peak efficiency of 17.7% at a cell thickness of 25 μm as indicated in Figure 1.

Figure 3 also gives the available photocurent, labeled as JPHOTO. This is the maximum short circuit current that can be collected if the p/n junction has the ideal rectangular current-voltage characteristics. It shows that there

is approximately 3 mA/cm^2 loss which is nearly constant as the thickness of the cell decreases. For perfectly reflecting back surface, both the JPHOTO and the JSC curves in Figure 3 would be higher but the increase is small even at 10 μm cell thickness. The difference is larger at smaller cell thickness, reaching a factor of two for very thin cells (less than one micron cell thickness).

(5) Fill Factor, FF

The fill factors of the various cells studied here are shown in Figure 4. The broken curves are those computed from the ideal analytical theory, using the exact open circuit voltages obtained from the transmission line circuit model calculations. The upper three broken lines are from the Shockley ideal low level diode theory, $I(Dark) = I_1[\exp(qV/kT) - 1]$ while the lower three broken lines are from the ideal high level diode theory, $I(Dark) = I_2[\exp(qV/2kT) - 1]$. One general trend is evident:- all the curves are below the ideal low level theory but substantially above the ideal high level theory. The thickness dependence of the fill factor is small for all the cells. This reflects the condition that cell thickness variation does not significantly alter the injection level. The thickness dependence is smaller for the cells with higher base doping (55131P and 55131N) which are also the cells with FF closest to the ideal low level theory. Even for the $5x10^{14}$ cm^{-3} base doping cells, the variation of the fill factor with thickness is small.

One important application of the fill factor is that it is an useful indicator of the current transport mechanism in the cell and whether there are series and shunt resistance problems in the cell construction.

The highest efficiency silicon cells thus far reported, p+/n/n+, 10 Ω-cm base [4], showed a measured fill factor very close to the 0.8 range covered by the 5412 and 5413 curves indicated in Figure 4. However, thin-film cells have given low FF (0.77 or less while expecting 0.83) suggesting complex recombination losses [5].

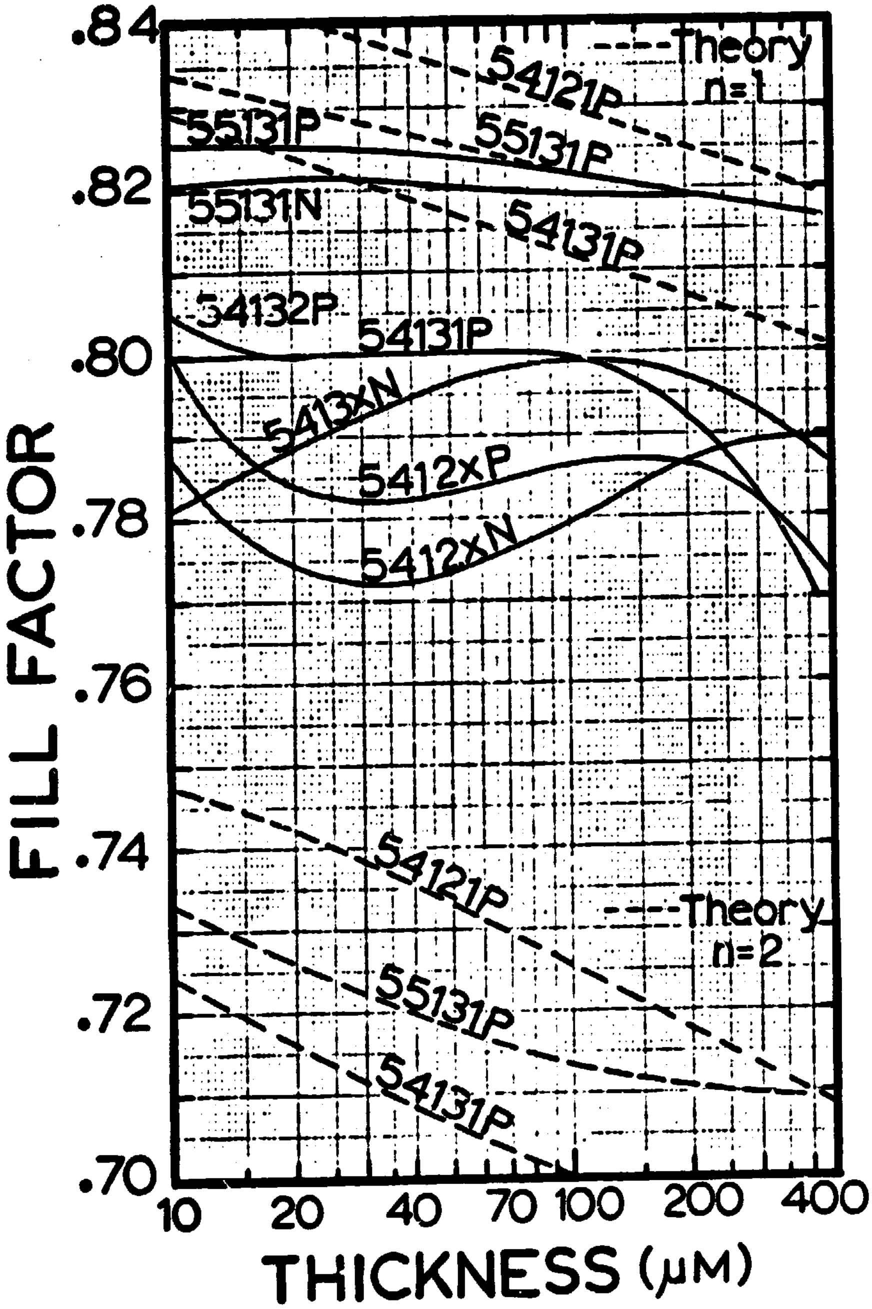

Figure 4 The fill factor as a function of thickness of silicon p/n junction solar cells under one AM1 sun illumination.

2.4 SUMMARY

A computer calculation has been made to investigate the thickness dependences of the performance of silicon thin film solar cells. The transmission line circuit model was used to solve the Shockley Equations without using analytical approximations to the solution. The two energy level double acceptor zinc recombination impurity center is used as the recombination model. Back surface field cells are considered since the back surface field improves the open circuit voltage substantially for thin cells while cells without the back surface field would have lower open circuit voltages for smaller cell thickness. Results of computed performance of about 100 cells under one AM1 sun condition show the following general trends. (1) The efficiency of the cell peaks around a cell thickness of about 50 μm, but the peak is very broad, covering as much as a three-to-one range of cell thickness with less than 1% efficiency variation at a peak efficiency around 17%. (2) The p+/n/n+ cell has a lightly higher efficiency than the n+/p/p+ cell, about 0.7% higher at 17% efficiency. This was shown to be primarily due to higher interband Auger recombination in the n+ region than in the p+ region due to the relatively constant phosphorus diffusion profile compared with the boron diffusion profile. (3) Two optical passes using a perfectly reflecting back surface will increase the short circuit current and efficiency by less than 1% (0.7% when comparing two n-base cells at about 17% efficiency) at the optimum cell thickness or peak efficiency in the 35 to 70 μm range. Performance improvement from two optical passes over one optical pass becomes more significant when the cell thickness drops below ten microns. For example, an improvement from 15.3% to 17.?% is predicted when a perfect reflecting back surface is added to a n-base, p+/n/n+ cell with 5×10^{14} cm^{-3} base dopant and 10^{12} Zn/cm^3 recombination impurity concentrations, whose thickness is 10 μm with a 0.25 μm emitter and 1.0 μm back surface field n+ layer. This is shown

by curves 54122N and 54121N in Figure 1.

For very thin cells with thickness below about 10 μm, the open circuit voltage becomes very high, as much as 700 mV. It comes from a lowering of the total recombination current in the base layer due to thinner base. Emitter recombination would become increasingly important in thin base cells and should become the limiting factor eventually for very thin cells. Another factor that limits the improvement of open circuit voltage achievable in thin film cells is the quality of the back surface field potential barrier of the n/n+ or p/p+ low/high junction. If this low/high junction is patchy, due to random occurrence of regions of low barrier or high recombination rates from defects and impurity clusters in aluminum-alloyed or diffused BSF junctions, then these patchy low/high junction regions can become ohmic which would greatly increase the base recombination current in thin-base BSF cells but would have little effect on the thick-base cells. These short-circuit patches across the BSF low/high junction would reduce the open-circuit voltage to a value much below that predicted for the thin-film BSF cells. An analysis based on an analytical model of perimeter and interior patches has been made and will be reported which shows that as much as 100 mV open circuit degradation is possible for cells which are electrically thin and small or cells with base thickness and edge dimension or diameter which are small compared with the minority carrier diffusion length in the base [5].

REFERENCES

1. C. T. Sah, P. C. H. Chan, C. K. Wang, R. L. Y. Sah, A. Yamakawa and R. Lutwack, "Effect of zinc impurity on silicon solar-cell efficiency," IEEE Transaction on Electron Devices, Vol. ED-28, 304-313, March, 1981.
2. J. M. Blocher, Jr., M. F. Browning and D. A. Seifert, "Evaluation of selected chemical processes for production of low-cost silicon," DOE/JPL 954339-80/20, December 19, 1980.
3. J. Dziewior and W. Schmid, "Auger coefficients for highly doped and highly excited silicon," Applied Physics Letters, Vol. 13, 346-348, September 1, 1977.
4. J. G. Fossum and E. L. Burgess, "High efficiency p+/n/n+ back-surface-field silicon solar cells," Applied Physics Letters, Vol. 33, 238-240, August 1, 1978.
5. C. T. Sah, to be published.